Int. J. Electrochem. Sci., 1(**2006**)447-455

International Journal of
ELECTROCHEMICAL
SCIENCE
www.electrochemsci.org

An Investigation on Metallic Bipolar Plate Corrosion in Simulated Anode and Cathode Environments of PEM Fuel Cells using Potential-pH Diagrams

*Yan Wang, Derek O. Northwood**

Department of Mechanical, Automotive, and Materials Engineering, University of Windsor,
401 Sunset Avenue, Windsor, Ontario, Canada N9B 3P4
*E-mail: dnorthwo@uwindsor.ca

Received: 3 September 2006 / *Accepted:* 25 September 2006 / *Published:* 1 December 2006

In order to reduce the price of the bipolar plates, many researchers have been developing metallic bipolar plates to substitute for the non-porous graphite bipolar plates. However, metallic bipolar plates corrode in the PEMFC environments and resultant metal ions can affect the conductivity of the membrane, and the performance of the fuel cell stack. In this study, the corrosion behaviors of three types of metallic materials (6061 aluminum alloy, A36 steel and Grade 2 titanium) in simulated anode and cathode environments of PEMFCs is analyzed using potential-pH diagrams. Potentiostatic electrochemical testing results and SEM metallography were used to verify the predictions of the potential-pH diagram. The results show that potential-pH diagrams can be used to predict the corrosion of these metals in the PEMFC conditions.

Keywords: Potential-pH diagrams, Corrosion, PEMFC, Bipolar plates, Durability

1. INTRODUCTION

Bipolar plates are one of the most important components in PEM (Proton Exchange Membrane) fuel cells. They are designed to perform many functions, such as: distribute the fuel and oxidant in the stack; facilitate water management within the cell; separate the individual cells in the stack; carry current away from the cell; facilitate heat management [1]. Currently, the main commercial bipolar plates are made of non-porous graphite because of its chemical and thermal stability. However, the high price of the non-porous bipolar plates prevents them from being widely used.

Metallic materials are thought to be one of the most promising candidates to substitute for non-porous graphite bipolar plates because of their good mechanical stability, electrical conductivity,

thermal conductivity and recyclability. Also, they can be easily and consistently stamped to the desired shape to accommodate the flow channels [1]. As a component in PEMFC, metal bipolar plates should have very high corrosion resistance because any metal ions generated from the corrosion process can migrate to the membrane, lower the ionic conductivity of the membrane, and thereby degrade the performance of the fuel cell stack. Moreover, any corrosion layer will lower the electrical conductivity of the bipolar plates and thus increase the potential loss of PEM fuel cells due to the high electrical resistance. At the anode and cathode, bipolar plates are at -0.1VvsSCE and 0.6VvsSCE, respectively [2]. Therefore, metallic bipolar plate corrosion under the PEMFC environments is different from free potential corrosion.

The potential-pH diagram is a map showing conditions of solution oxidizing power (potential) and acidity for the various possible phases that are stable in an aqueous electrochemical system. The boundary lines on the diagram, which divide areas of stability for the different phases, are derived from the Nernst equation. Potential-pH diagrams have been used in many applications, including fuel cells, batteries, electroplating, and extractive metallurgy [3]. We believe that this is the first time that potential-pH diagrams have been used to predict the corrosion of the metallic bipolar plates under the PEMFC working conditions.

2. POTENTIAL-pH DIAGRAMS AND EXPERIMENTAL DETAILS

2.1 Potential-pH diagrams

The potential-pH diagrams for the three different metal electrodes using the Nernst equation.

2.2 Electrode preparation and electrochemical measurements

Three alloys were chosen as the base material, namely, 6061 aluminum alloy, A36 steel and pure titanium (grade 2). The chemical analysis of the Al6061 and A36 steel are given in Table1.

Table 1: Chemical compositions of Al6061 and A36 steel (wt%)

Metal	C	Mn	P	S	Si	Cr	Cu	V	Ti	B	Ca	Mg	Zn	Ga	Al	Fe
Al6061	_	_	_	_	0.70	0.18	0.25	_	_	_	_	1.12	0.02	0.02	balance	0.46
A36	0.06	0.12	0.004	0.005	0.09	0.02	0.01	0.003	0.003	0.0001	0.0019	_	_	_	0.047	balance

The metals were received in sheet form. The sheets were cut into samples of dimensions 1.5cmx1.5cm (area is 2.25cm^2). An electrical contact was made to one side by means of nickel print. Then the contact side and the edges of the metal sample were sealed with epoxy resin, leaving one side for the electrochemical tests and characterization [2]. In the corrosion tests of the metallic bipolar plate materials, the samples were polished using 240,600,800 grit silicon carbide papers followed by 1.0μm alumina powder. In order to simulate the working conditions of PEMFCs, potentiostatic tests were conducted. At the anode, the applied potential was -0.1VvsSCE purged with H_2 and at the cathode, the applied potential was 0.6VvsSCE purged with O_2. The test temperature was 70ºC since the working temperature of PEMFC is 70ºC ~100ºC [4]. The electrolyte was a 0.5M H_2SO_4 solution.

2.3 Metallographic Characterization

In order to characterize any corrosion products of the metals, the surfaces of the corroded samples were examined by scanning electron microscopy (SEM) [JEOL JSM-5800LV].

3. RESULTS AND DISCUSSION

3.1 Potential-pH diagrams

In the PEMFC working environments, the anode and cathode are at different potentials, which is different from free potential corrosion. Potential-pH diagrams are an excellent tool to research metal corrosion at the different pH values and potentials. Because 5~10ppm metal ions can affect the ionic conductivity of the membrane, and thus the performance of the fuel cell stack [5, 6], we assume that the metal ion concentration is 10ppm in the simulated PEMFC environments when drawing the potential-pH diagrams. Based on the Nernst equation and assumption that the three alloys are essentially Al, Fe and Ti, potential-pH diagrams have been constructed and are shown in Figures1~3 [3]. In the PEMFC working environment, pH is in the range 0~3.5 [7, 8]. At the anode, the potential of the bipolar plates is -0.1VvsSCE and at the cathode, the potential of the bipolar plates is 0.6VvsSCE. This information can be used to predict the behaviour of Al6061, A36 steel and Grade 2 Ti as metallic bipolar plates in PEM fuel cells.

From Fig1, we can see that Al^{3+} is the stable form for Al at -0.1V when the pH is 0~3.5. Thus, at the anode, Al will corrode and form Al^{3+}. At the cathode, we can see that Al^{3+} is also the stable form for Al. Therefore, wherever it is at the anode or the cathode as the metallic bipolar plates, Al is always corroded and the corroded product is Al^{3+}. Therefore, Al is prone to corrode in the PEMFC working conditions and can not be used as bipolar plates without some form of protective coating.

From Fig2, we can see that Fe^{2+} is the stable form at the anode when pH is 0~3.5. At the cathode Fe^{3+} is the stable form at pH 0~3.28 and $Fe(OH)_3$ can be formed between pH 3.28 and 3.5. So Fe can be corroded at both the anode and cathode, however, Fe^{2+} is the corrosion product at the anode and Fe^{3+} is the corrosion product at the cathode. When the pH value is larger than 3.28, $Fe(OH)_3$ will be formed.

From Fig3, we can see that TiO_2 is the stable form of Ti at the anode and TiO_2 is also the stable form of Ti at the cathode. Ti will be oxidized in the PEMFC conditions and there is no corrosion of Ti bipolar plates. However, even if there is no corrosion on the Ti surface, TiO_2 can affect the performance of the bipolar plates because the oxide will increase the contact resistance between the Ti bipolar plates and gas diffusion layers.

In summary, Al will corrode at the anode and the cathode in a PEMFC working environment and the corrosion product is Al^{3+} ions. Fe corrodes at the anode and the cathode in a PEMFC working environment and the corrosion product is Fe^{2+} ions at the anode and Fe^{3+} ions at the cathode. Ti is oxidized at the anode and cathode rather than corroded and the product is TiO_2. However, in a 'real' PEMFC, the working potential can fluctuate over a potential range. For example, short-term local voltage can exceed 1V under start conditions if oxygen gains access to the anode side of the fuel cell [9, 10]. If the working potential is below to -0.113V, Ti will corrode to form Ti^{3+} ions.

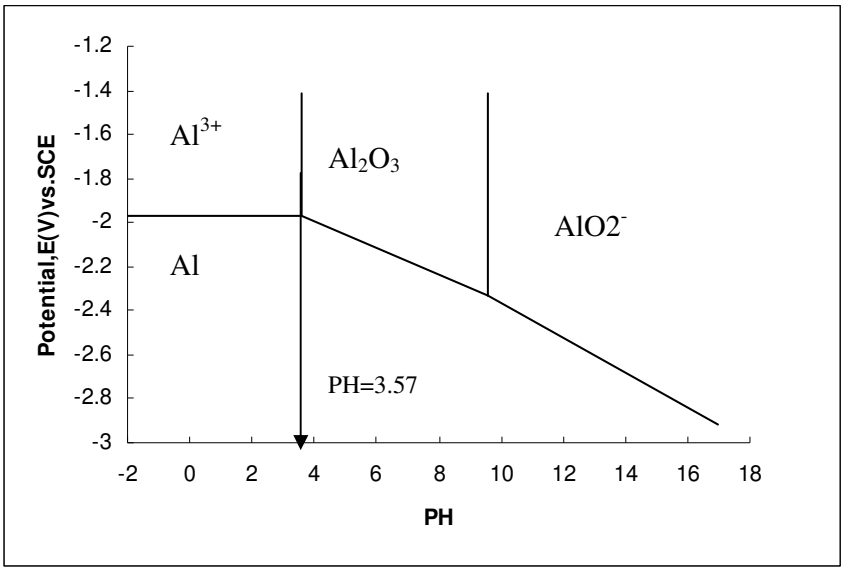

Figure 1. Potential-pH diagram for Al

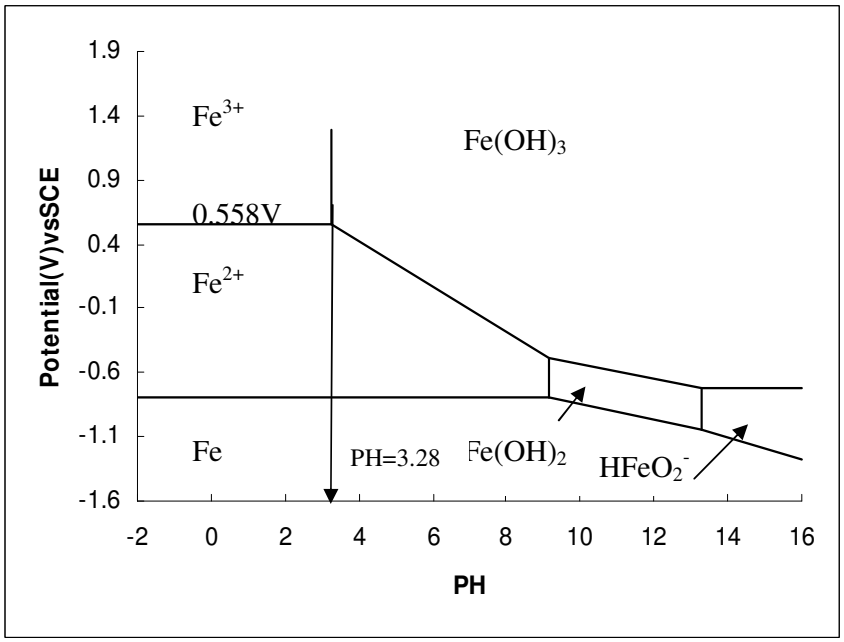

Figure 2. Potential-pH diagram for Fe

3.2 Potentiostatic results

In order to confirm that potential-pH diagrams can actually be used to predict the corrosion of the metallic bipolar plates in the PEMFC working environment, potentiostatic electrochemical tests were conducted. Figs4 and 5 [11] show the potentiostatic test results for the three metals in the simulated anode and cathode environments. Because the electrolyte is a 0.5M H_2SO_4 solution, the pH

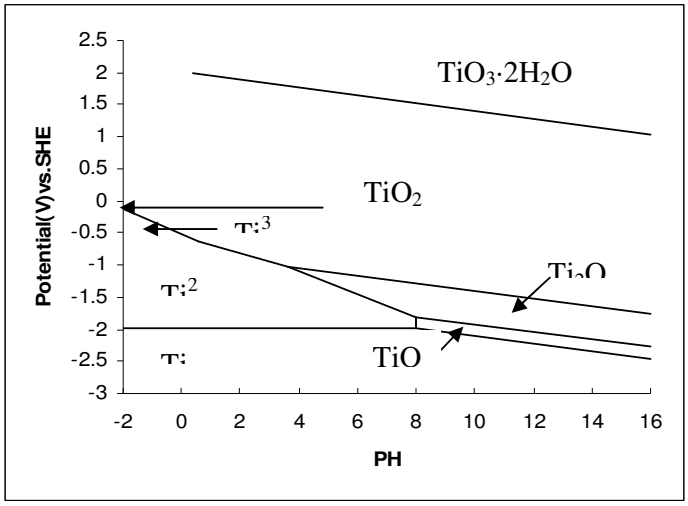

Figure 3. Potential-pH diagram for Ti

of the solution is 0. From Fig4, we can see that Al6061 and A36 steel corrode and the corrosion current density is $4x10^{-3}A/cm^2$ for Al6061 and $6x10^{-3}A/cm^2$ for A36 steel in the simulated anode conditions. However, the corrosion current density of Ti is very small and is gradually reduced to a negative value after about 1500 seconds. The initial positive current is due to the oxidization of Ti. The subsequent negative current is due to the reduction of H^+, which supplies the cathodic protection for Ti [11]. After one hour, the current density maintains at about $-8x10^{-6}A/cm^2$. Therefore, in the simulated anode environments of PEMFC, Ti is first oxidized, and then a negative current provides protection. From Fig5, we can see that both Al6061 and A36 steel are corroded in the simulated cathode conditions and that the corrosion current density is $3x10^{-4}A/cm^2$ and $8x10^{-5}A/cm^2$ respectively, after one hour. It can be seen that the corrosion current density suddenly drops after about 1000 seconds for both Al6061 and A36 steel. This is because of concentration polarization: a detailed explanation can be found in ref [11]. The corrosion current density for Grade 2 Ti is $2x10^{-5}A/cm^2$. Comparing the results in the anode and cathode conditions, the corrosion current is higher in the cathode environment than in the anode environment for both Al6061 and the A36 steel. For Ti, the oxidation rate is higher in the cathode environment than in the anode environment, and there is no oxidization at the anode side after 1500 seconds.

3.3. SEM results

Fig6 presents SEM micrographs of the corroded surfaces of Al6061 under anode and cathode conditions. From Figs6a and 6b, we can see that Al6061 corrodes through both pitting corrosion and intergranular corrosion at the anode. From Fig6c, we can see that there are some large holes in the Al6061 surface on the cathode side. If we examine these larger 'hole' areas at a higher magnification, Fig 6d, we can see that the aluminum matrix has been preferentially etched out, exposing the second phase particles within the microstructure. Similar observations were made at the cathode side for regions of the sample that did not contain the larger 'hole' areas, Fig 6e.

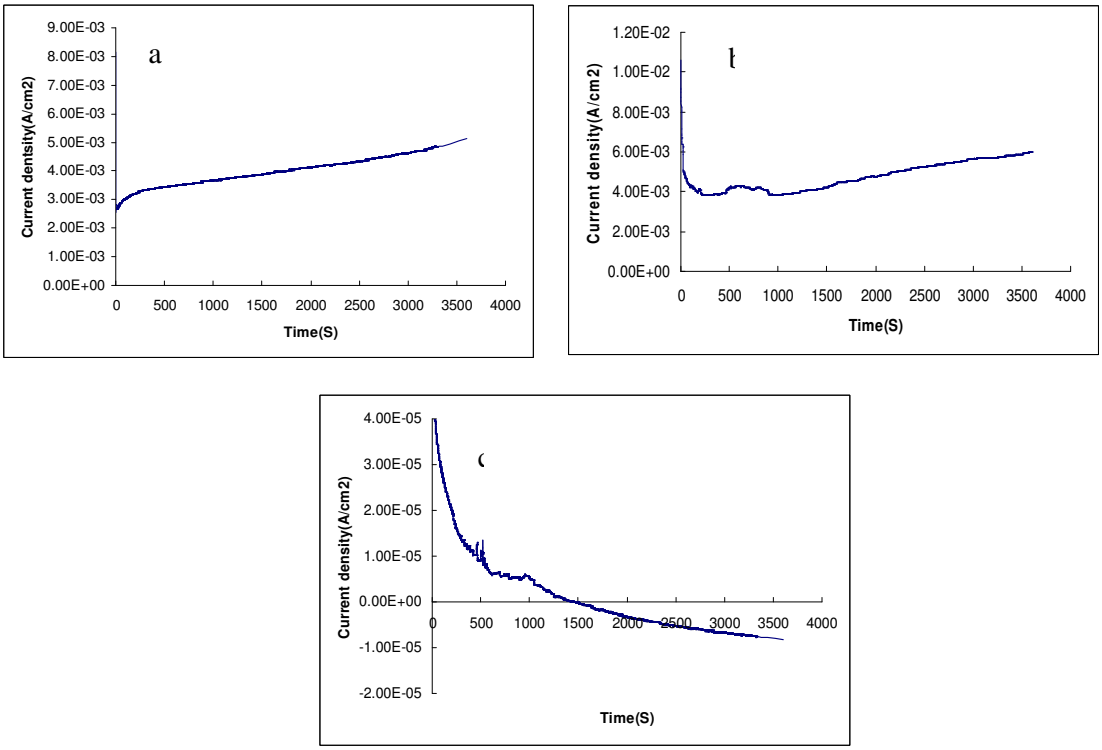

Figure 4. Potentiostatic tests in the simulated anode environments, (a) Al6061, (b) A36 steel, (c) Grade 2 Ti

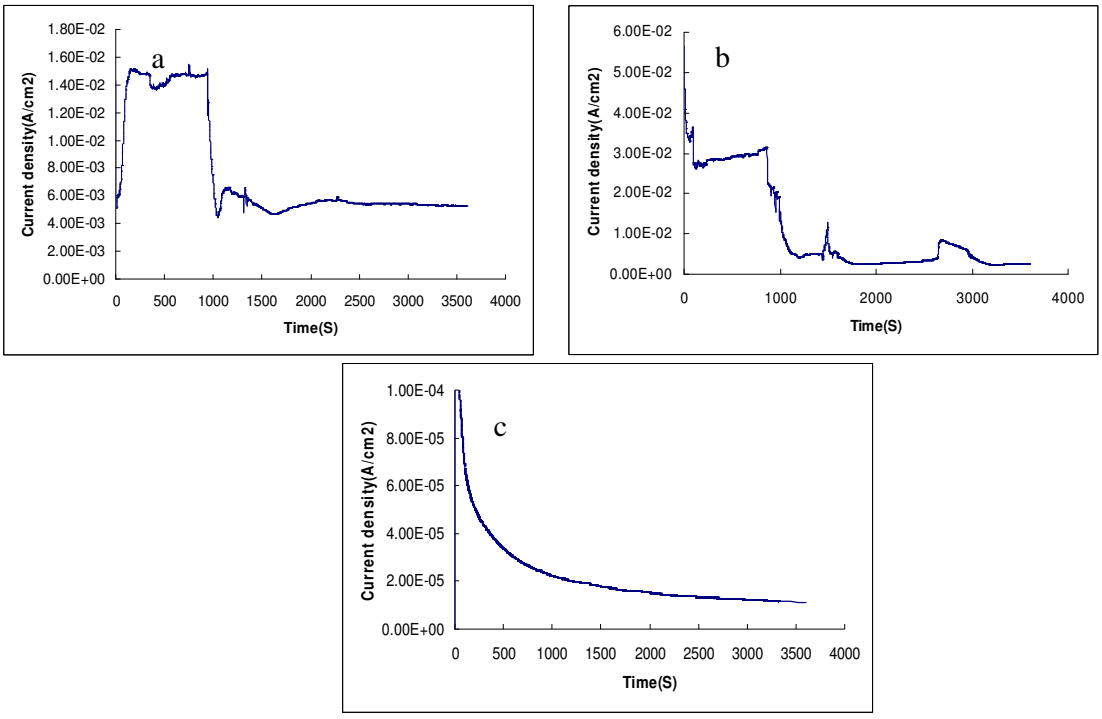

Figure 5. Potentiostatic tests in the simulated cathode environments, (a) Al6061, (b) A36 steel, (c) Grade 2 Ti

From some researches [12], the precipitate phase is either Al-Mg-Si or Fe-Al-Cr. Comparing the anode and cathode corrosion of Al6061, we found that corrosion in the cathode conditions is more severe. This is because the simulated cathode potential is 0.6VvsSCE and the simulated anode potential is -0.1VvsSCE. The corrosion potential for Al6061 is -0.7VvsSCE, and so the simulated cathode potential is more oxidative. From the potential-pH diagram, Fig1, we know that the corrosion products are Al^{3+} at both the anode and cathode sides.

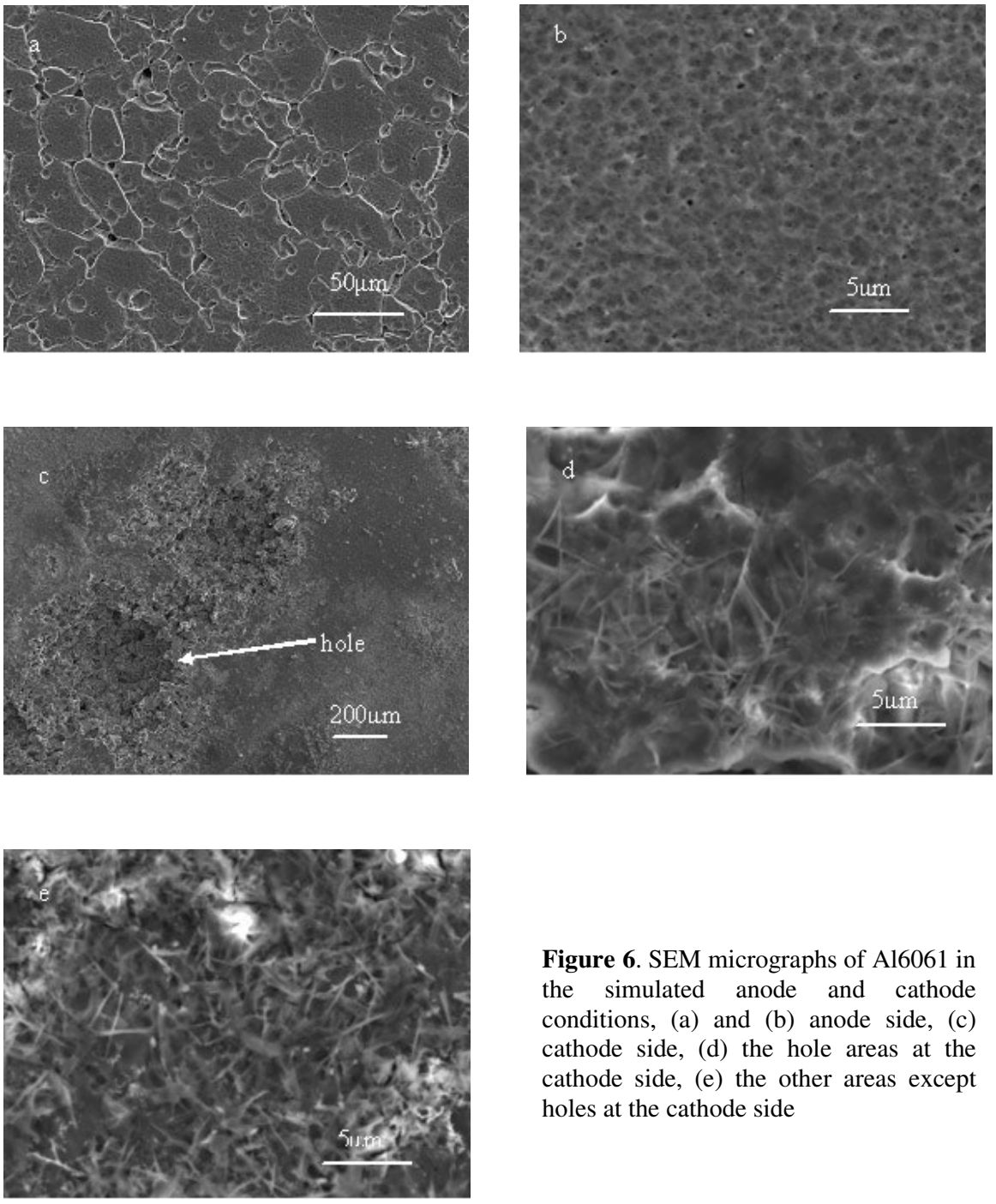

Figure 6. SEM micrographs of Al6061 in the simulated anode and cathode conditions, (a) and (b) anode side, (c) cathode side, (d) the hole areas at the cathode side, (e) the other areas except holes at the cathode side

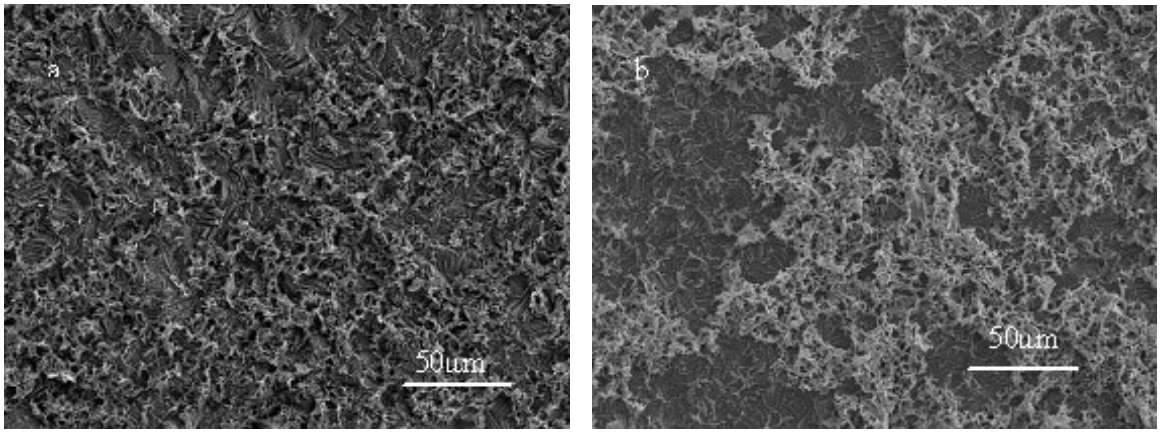

Figure 7. SEM micrographs of A36 steel in the simulated anode and cathode conditions, (a) the anode side, (c) the cathode side

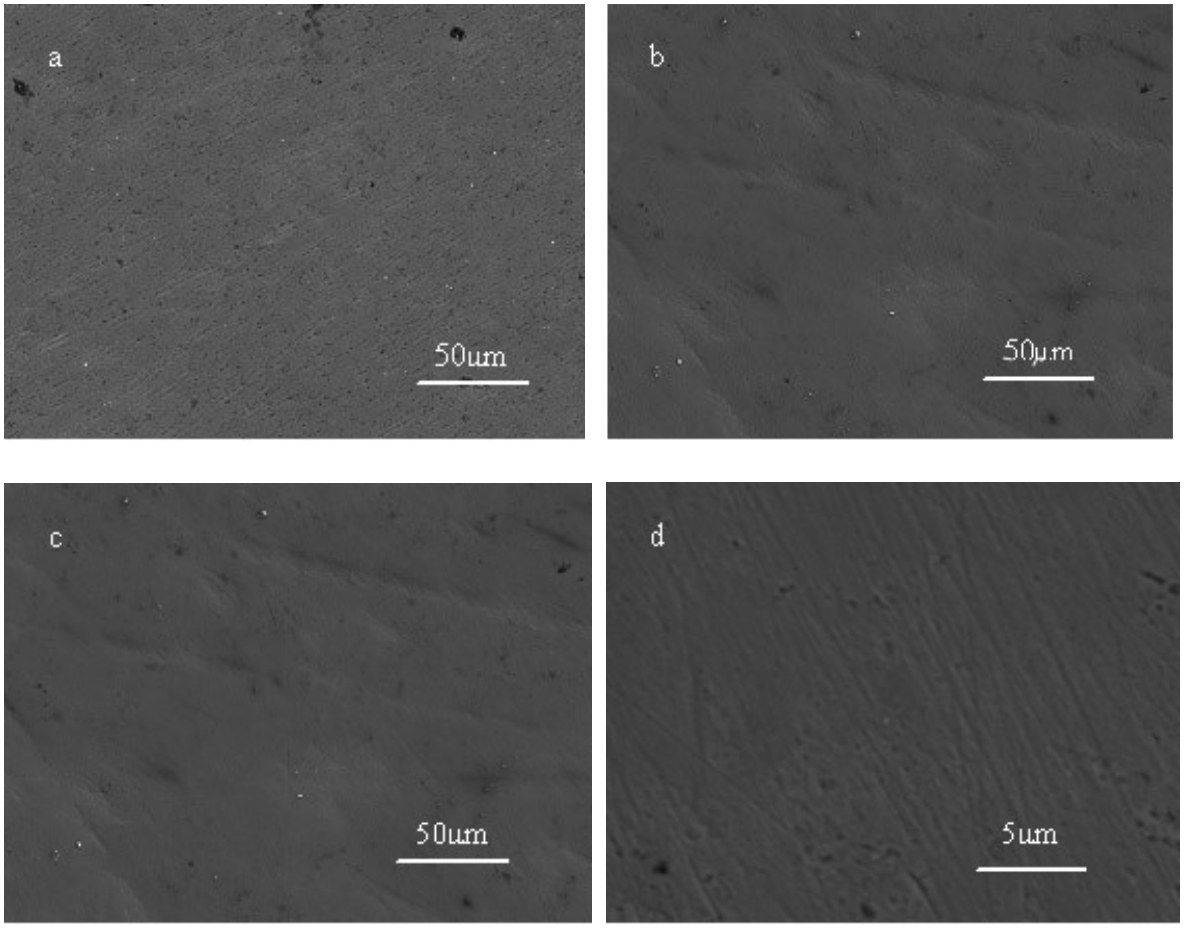

Figure 8. SEM micrographs of Ti in the simulated anode and cathode conditions, (a) and (b) the anode side, (c) and (d) the cathode side

4. CONCLUSIONS

Potential-pH diagrams can be used to predict the corrosion behaviour of the metallic bipolar plates under PEMFC working conditions. The results of both the potentiostatic testing and SEM metallography are consistent with the predictions from the potential-pH diagrams. Al alloy 6061 corrodes at both the anode and cathode in a PEMFC working environment and the corrosion product is Al^{3+}. A36 steel (Fe) corrodes at the anode and cathode in a PEMFC working environment and the corrosion product is Fe^{2+} at the anode and Fe^{3+} at the cathode. Grade 2 Ti is oxidized at both the anode and cathode and the oxidation product is TiO_2, which is harmful to the PEM fuel cell performance because it will increase the contact resistance. Although potential-pH diagrams predict the stable phases for given values of potential and pH in simulated PEMFC conditions, they give no information on the rates of any corrosion reactions.

ACKNOWLEDGES

The authors would like to thank Mr John Robinson for his assistance with the SEM examination. The research was financially supported by the Natural Sciences and Engineering Research Council of Canada (NSERC) through a Discovery Grant awarded to Professor Derek O. Northwood.

Reference:

1. A.Hermann, T.Chaudhuri, P.Spagnol, *Int.J. Hydrogen Energy*, 30(2005)1297.
2. H.Wang, J.A.Turner, *J.Power Sources*, 128(2004)193
3. D.A.Jones, Principles and Prevention of Corrosion, Macmilian, New York (1992)
4. M.A.Laughton, *Power Engineering J*, 16(2002)37
5. L.Ma, S.Warthesen, D.A.Shores. *J.New Mater Electrochem Sys*, 3(2000)221
6. M.P.Brady, K.Weisbrod, I.Paulauskas, R.A.Buchanan, K.L.More, H.Wang, M.Wilson, F.Garzon, L.R.Walker, *Scripta Materialia*, 50(2004)1017
7. S.Lee, C.Huang, J.Lai, Y.Chen, *J.Power Sources*, 131(2004)162
8. ASTM G5-94, Standard Reference Test Method for Marking Potentiostatic and Potentiodynamic Anodic Polarization Measurements, American Society for Testing and Materials, Philadelphia (1995)
9. C.A.Reiser, L.Bregoli, T.W.Patterson, J.S.Yi, J.D.Yang, M.L.Perry, T.D.Jarvi, *Electrochemical and Solid State Letters*, 8(6)(2005)A273
10. M.P.Brady, B.Yang, H.Wang, J.A.Turner, K.L.More, M.Wilson, and F.Garzon, *J. Minerals, Metals & Materials Society* ,58(8)(2006)50
11. Y.Wang, D.O.Northwood, An Electrochemical Investigation of Potential Metallic Bipolar Plate Materials for PEM Fuel Cells, Presented at International Symposium on Solar-Hydrogen-Fuel Cells, Cancun, Mexico, August 20-24,2006
12. M.A.Alodan and W.H.Smyrl, *J. Electrochem. Soc*, 145(1998)1571